SUPERCONDUCTING MATERIALS-A REVIEW OF RECENT ADVANCES AND CURRENT PROBLEMS IN PRACTICAL MATERIALS

David C. Larbalestier

Abstract - In the four years since the last International Magnet Technology Conference, there has been a significant increase in both the breadth and scale of superconducting magnet construction. A number of advances have been pursued out of the laboratory into large scale construction so that today we see large scale magnets utilizing He I in free convection boiling, He I in conduit (force flow) and He II. Whereas four years ago filamentary Nb_3Sn had only just become available in magnet conductor configurations and lengths, now it is being produced in quantity for a number of large projects. The discontinuous route to filamentary Nb_3Sn has received much laboratory investigation and may soon be available for industrial scale production. Fundamental studies of Nb_3Sn and other A15 compounds have shown that significant improvements in J_c and H_{c2} are possible, although not all improvements can be achieved with favorable fabrication techniques. There have also been substantial developments in Nb-Ti. Production has increased significantly and experience with large scale production runs has assisted the development of higher J_c values in both the small diameter, fine filament conductors typical of high energy physics magnets as well as the large monolith, large filament conductors utilized for some MHD and fusion applications. Microstructural-processing studies have begun to reveal some of the crucial steps in the optimization of conductors of arbitrary size and design. At the same time it has proved possible to raise the upper critical field of Nb-Ti by alloying, particularly with Ta, and these alloys may find significant application in magnets of 8-12 Tesla for applications such as fusion, new higher energy accelerators and NMR. This paper reviews these and other important developments in the field of practical superconducting materials.

I. INTRODUCTION

To attempt a survey of recent advances and current problems in practical superconducting materials is an undertaking of considerable magnitude, given the diverse nature of the present applied superconductivity community. In order to make my task at least reasonably manageable, I have confined my comments to Nb-Ti and Nb_3Sn, knowing that other materials will be discussed in a companion paper at the Workshop on the Frontiers of Technology in Superconducting Materials for Magnets[1]. There is, however, plenty to discuss for both of the above materials and the rapid increase in the scale of production seen for these materials is plainly throwing up many questions to which we do not yet have the answer.

One of the immediately obvious changes which has occurred since the last Magnet Technology Conference 4 years ago has been a major increase in the size of the market for superconductors and the scale and organizational changes that have occurred in the superconducting wire industry as a result. Market surveys of all sorts have been made and there has indeed been a large increase in industry turnover and in the number and scale of the end markets for the superconductor. A characteristic of some of these new markets, for example fusion and MHD, is the fact that, however important the magnets are in the overall devices, solution of the magnet problems is by no means the most important part of the project. In other words, there has been a distinct change of emphasis to a situation where the business is now driven by the large scale industrial fabricator of the magnet instead of by the intrinsic scientific interest of the research laboratory.

At the outset of the preparation of this paper I attempted to step a little outside my usual role as a scientific investigator of the superconductor and to imagine what might be some of the questions posed by a technically competent newcomer to the business who was placing the order for a large conductor procurement for a major new magnet system. Some of the questions imagined were:

(i) Can this conductor be made reliably by several manufacturers and can it be bid realistically in open competition?

(ii) Can I scale the current density from a standard critical current density plot and expect to get about the same values in my particular design of conductor?

(iii) How long a piece length can be made?

(iv) How long do I have to wait for delivery?

(v) What prospects are there of expecting either a modest improvement in properties and/or a modest reduction in price (say of order 10%) without technical input from my staff?

(vi) Does scrap magnet wire have any value?

There have been many cases of the single source, cost plus fee type contract response to these questions but also many cases in which conductors have been bid from one or more sources at a fixed price. Although there have been many successful procurements, there have also been sufficient failures or unexplained features of successful production to provide ample evidence that basic features of composite fabrication and property prediction lack quantitative definition. In general, however, the superconductor fabrication community has not been good at cataloguing its failures or even describing its successes in detail. Our colleagues, the magnet builders, are perhaps more forthcoming: Bruce

The author is with the University of Wisconsin, Materials Science Program, Madison, WI 53706, USA.

0018-9464/81/0900-1668$00.75

Montgomery reviewed[2] a number of significant magnet failures some years ago and the tribulations of the recent TPC magnet are described by Green et al.[3] in a companion paper at this conference. This lack of discussion handicaps our efforts to understand the complex fabrication-microstructure-property relationships, many of whose quantitative details still remain obscure.

The plan of the present review is to select certain topics relating to recent advances or current problems. A broader perspective may be obtained from reviews in the recent ICMC conferences[4,5], the 1980 NATO Advanced Study Institute on Superconducting Materials[6] and the 1980 Applied Superconductivity Conference[7]. This author has provided two long reviews on Nb-Ti[8,9], Suenaga two on filamentary Nb_3Sn[10,11], Hillmann one on fabrication aspects of both Nb-Ti and Nb_3Sn[12], while stress effects in the A15 compounds have been reviewed by Welch[13] and Ekin[14]. In situ conductors have received several reviews[15-19], while the basic phase relationships of the A15 compounds have been reviewed by Flukiger[20].

II. GENERAL CONSIDERATIONS

One of the questions of increasing importance is that of standards and specifications. This is natural as the superconductor business leaves its research laboratory background to become an established high technology industry. One area of standards concern is that of defining critical current, another that of defining a chemical specification with permitted impurities for the raw material Nb or Nb-Ti. Successful standards will permit competent scientists and engineers, who are not themselves specialists in superconductivity, to safely specify materials and tests. However, formulation of such standards is not necessarily easy, even when the experts agree on the technical details (I believe this to be broadly the case in the case of a critical current standard), since the implications of too stringent a test may be considered financially prohibitive. Things are even more uncertain, for example, in respect of superconductor composition, since the scientific aspects of permitting greater freedom in the chemical composition are unknown. There are of course many other specifications, most quite local in application, affecting the supply and delivery of superconductor. Some of these specifications date from the very early days in superconductor manufacture and it may, therefore, be helpful periodically to ask the questions:

(i) What situations or contingencies are these specifications supposed to ensure or avoid?

(ii) Is there a good scientific or empirical base to justify the specifications?

My purpose in raising this point is to attempt to focus attention on the quantitative and predictive aspects of our knowledge, rather than the purely qualitative and general. For example, we understand quite well that lots of cold work and the correct heat treatment are desirable for Nb-Ti composites. But the actual fabrication of particular composites follows a recipe which is generally secret and essentially empirical. Small changes in composite design frequently lead to considerably different properties and yields and a general concern of U.S. wire manufacturers is product variability, even given the rather stringent specification of the initial Nb-Ti.

To understand why this is so we need look no further than the connection between what the fabricator does to his composite extrusion billet and the properties that he measures before he ships it out the door. Present emphasis is on large scale production. Superconductor billets now weigh 1/4 to 1/3 ton, with starting diameters of 25 to 30 cm. Annual Nb-Ti production in the USA is about 100 tons of alloy per year and over 800 nominally identical billets of the Fermilab Energy Saver/Doubler composite (Fig. 1) have been made. Large production facilities have come into operation and many magnets been constructed.

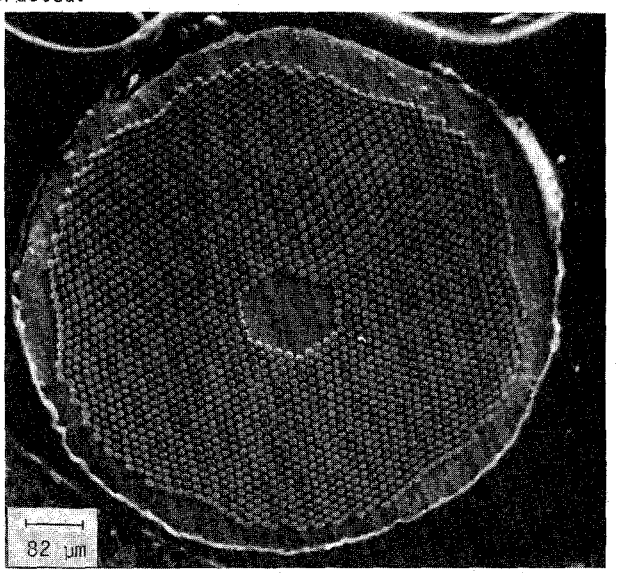

Fig. 1. Cross-section of a Fermilab composite.

If we inquire what is the mediator between the large scale fabrication equipment and the hopefully inexpensive, high quality, high current density conductor output, we shall find that this is the microstructure and its scale has not changed at all, remaining very fine in scale. The microstructure which pins the vortex lattice must be made heterogeneous on a scale comparable with that of the vortex lattice. For both Nb-Ti and Nb_3Sn, the vortex diameter is of the order 10nm (100Å). The equilibrium separation of the vortices depends on field as $(\phi_0/B)^{1/2}$, where ϕ_0 is the flux quantum, 2×10^{-15}Wb/m^2, and B is the magnetic field strength. The separation thus varies from about 40nm at 2T to about 15nm at 10T. The fabrication process will not produce a high critical current density unless it produces a microstructure on this scale. Such microstructures can be extremely complex. Figure 2 shows a high magnification transmission electron micrograph of a small part of a very high current density filament (J_c 10^{-14}Ωm, 5T,4.2K=2600A/mm^2)[21]. The microstructural defects here are the very high density of dislocations intro-

duced by the cold-drawing process. They have banded themselves into walls, forming a sub-band structure elongated along the drawing axis and possessing a characteristic separation of about 40nm. Not visible in the micrograph, but of crucial importance to the J_c, are precipitates of a normal (ie, non-superconducting) α-Ti phase produced by special heat treatments near the final wire size. The micrograph of a Nb_3Sn filament[22], in this case a transverse section normal to the drawing axis of the original Nb, appears somewhat simpler, (Fig. 3). In this case much of the dislocation structure existing in the Nb is annealed away during the high temperature reaction necessary to produce the Nb_3Sn. So far as we know, the Nb_3Sn that grows is single phase and the defect responsible for the high J_c is the grain boundary. A crucial parameter is then the heat treatment since this controls the grain size, which should be around 100nm or less if the J_c is to be high.

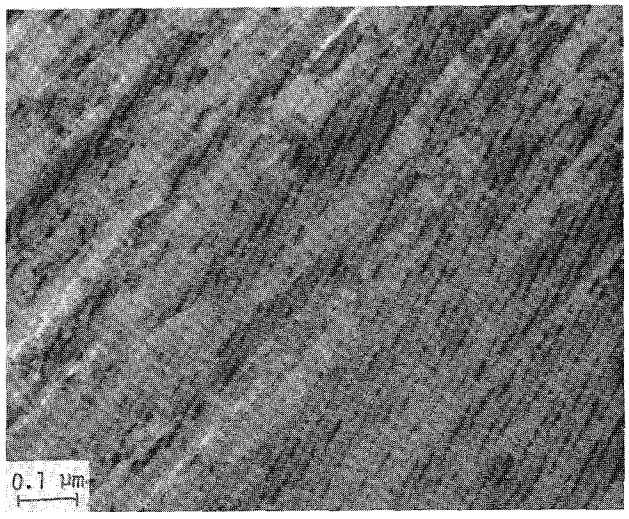

Fig. 2. Longitudinal section of a high current density Nb 50w/o Ti filament[21].

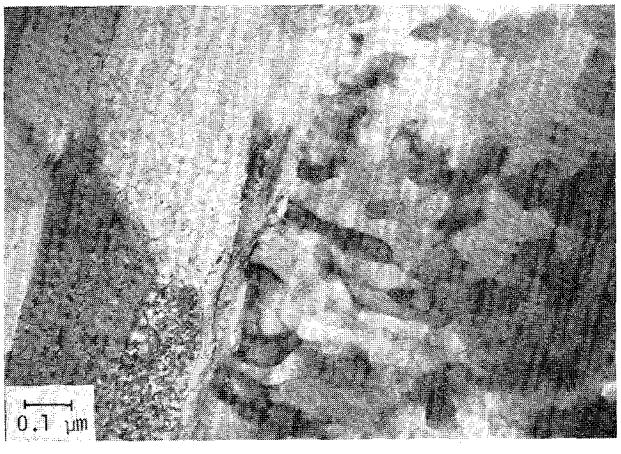

Fig. 3. Transverse section of a high current density Nb/Nb_3Sn filament. The Nb/Nb_3Sn interface runs down the middle of the micrograph[22].

This introduction of the microstructure at this stage serves to make several points:

(i) The microstructure is defective on a very fine scale and contains defects of high specific energy whose scale and distribution are critically sensitive to thermal treatment.

(ii) The microstructures of high J_c composites are of necessity inhomogeneous and because many of our common probes of the superconducting state, such as the resistive and magnetic measurement, respond preferentially to the regions of best superconducting property, we do not necessarily get a good picture of the volume distribution of the property from our measurement[23].

(iii) The fine scale of the defects, typically 10 to 100nm, requires sophisticated and non-routine methods of analysis, such as transmission electron microscopy.

It is perhaps for these reasons that many important production aspects of the fabrication of multifilamentary superconducting composites remain unclear. In a quantitative and predictive sense, our ignorance is still large. If we could risk a comparison with steel, we might say that although the empirical achievements of the industry have been considerable, our process control is still at the stage of "heat to cherry red, quench into sheep dip and reheat to pale straw - and for really important deliveries it wouldn't hurt to get the phase of the moon right too".

III. NIOBIUM-TITANIUM AND ITS ALLOYS

Upper Critical Fields

The upper critical fields of the binary Nb-Ti alloys are still a subject for discussion. A compilation of values from the literature is shown in Fig. 4[8,9] where, for example, $\mu_0 H_{c2}(4.2K)$ values of 12.4 Tesla have been claimed. Some of this confusion, particularly in older work, can be laid at the use of pulsed fields with short rise times and some to the use of differing definitions of H_{c2}. A more basic problem, however, is the fundamental heterogeneity of the optimized, high J_c superconductor, already discussed. T_c and H_{c2} are almost invariably measured by magnetic or resistive means. In the case of Nb-Ti and the ductile alloys the upper limit to the transition is believed to be determined by the short circuit paths of the sub-band structure and concentration gradients and other inhomogeneities are known to be present in diffusion grown layers of Nb_3Sn[23,24,25].

The upper critical field is most frequently measured resistively, with some small but arbitrarily chosen current density. In cold worked alloys a broad transition of 0.5-1 Tesla width is generally found (Fig. 5) and the position of the transition can vary over a similar range depending on the exact, even if negligibly small, measuring current density chosen. The investigator can in addition decide to report either the first departure from superconductivity, the disappearance of the last lingering trace or the transition mid-point. An alternative definition, which has some practical validity, is to use an extrapolation function of current density and field. For Nb-Ti and its alloys, this is just the bulk pinning

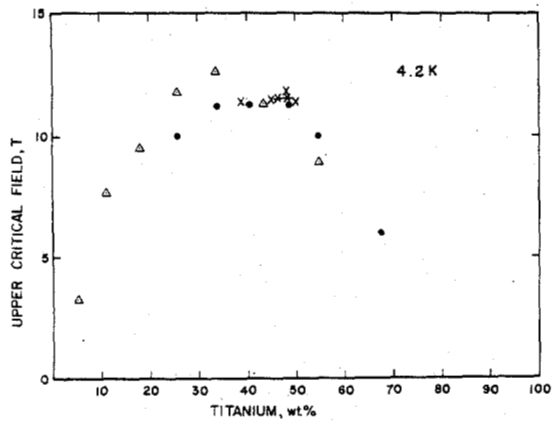

Fig. 4. Literature values of $\mu_0 H_{c2}$(4.2K) for Nb-Ti[9].

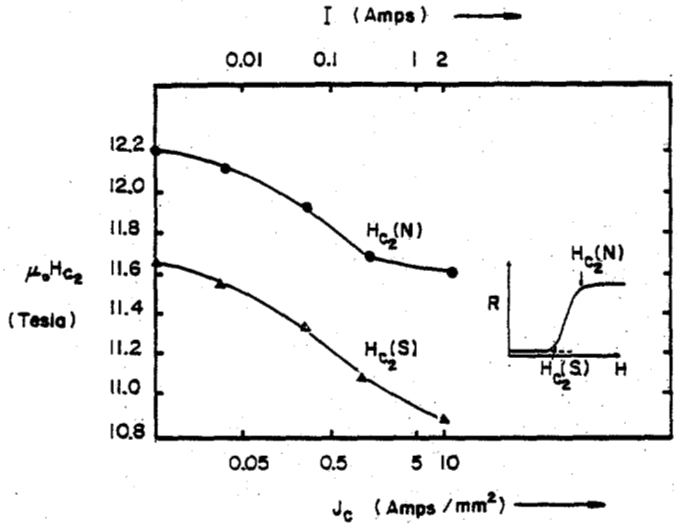

Fig. 5. Resistive H_{c2} transitions in cold worked Nb-Ti alloys[28].

force $F_p (=J \times B)$ [26], while for Nb_3Sn the Kramer function $J_c^{1/2} B^{1/4}$ is more usual[27]. Annealing the material should, in principle, remove the heterogeneity and produce a sharp transition characteristic of the bulk material. A comparison of the H_{c2} values obtained for Nb 46.5 w/o Ti under different conditions is shown in Table 1. There is seen to be a spread of 0.85 Tesla or about 8% in the H_{c2} values. It should be noted that the linear extrapolation to zero is a very good one[26]. Our conclusion is that an unambiguous definition of H_{c2} is difficult and that further work is needed with techniques that measure the actual volume fraction transforming before the situation will be fully explained.

With this understanding in mind it is possible to rationalize, if not completely understand, some of the claims made for high field superconductivity in Nb-Ti and its alloys. Two claims in particular stand out. One in the Nb-Ti-Zr system by Alekseevski et al.[29] for a $\mu_0 H_{c2}$(4.2K) value of 13.6T and one by Horiuchi et al.[30] for 13.1T in the Nb-Ti-Ta-Zr system.

Table 1

Measured $\mu_0 H_{c2}$(4.2K) Values for Nb 46.5 w/o Ti[28]

Experimental alloy as drawn 100:1 area reduction (J_c = 0.05 A/mm², definition as in Fig. 5)	11.5T
Experimental alloy annealed 20 mins/1350°C (J_c = 0.05 A/mm², by definition as in Fig. 5)	11.25T
Multifilamentary composite (J_c x B extrapolated linearly to zero)	10.65T

Remakes of these and neighboring alloys in our laboratory[28,31] produced maximum values of $\mu_0 H_{c2}$(4.2K) of 11.0 and 11.85T, respectively, using even the most optimistic definition of H_{c2}. Using our preferred definition (the first departure from the superconducting state at J_c=0.05 A/mm², a value at which H_{c2} is becoming insensitive to J_c, as shown in Fig. 5), the values are 9.7 and 11.25T, values which are not superior to those found in the binary Nb-Ti system[8,9,31]. When we first began to become interested in the high field properties of Nb-Ti about 3 years ago, we were surprised at this variability and the lack of precise quantitative understanding even for pure Nb-Ti alloys. Before discussing our alloy development work, however, it may be helpful to summarize some aspects of the theory of the upper critical field.

The theoretical framework for the understanding of the upper critical field is in principle well established. The basic equation is that of Ginzburg, Landau, Abrikosov and Gorkov (GLAG). The zero temperature predicted H_{c2}, $\mu_0 H_{c2}^*(0)$, is given by

$$\mu_0 H_{c_2}^*(0) = 3.11 \times 10^3 \, \rho_n \gamma \, T_c \quad \text{(Tesla)} \qquad (1)$$

where ρ_n is the normal state electrical resistivity and γ the electronic specific heat coefficient which is proportional to the density of states. For high-field, practical superconductors the constant of proportionality needs to be modified to take account of orbital paramagnetism, spin-orbit scattering, electron-phonon and electron-electron coupling effects[32,33]. In the binary Nb-Ti alloys, $\mu_0 H_{c2}^*(0)$ is not reached, due to limitations imposed by the orbital paramagnetism of the normal state; the GLAG value at 0K should reach ~18 Tesla instead of the ~15 Tesla experimentally observed. A more detailed discussion of these points has been given in 2 earlier review papers[8,9].

Several avenues appeared possible for alloy development aimed at increasing H_{c2}[28]. In terms of the GLAG equation, ρ_n is a parameter of significant structure sensitivity and the resistivity of the Nb-Ti alloys (as for all Group IV-V alloys) is anomalously high, due to the incipient lattice instability of the body centered cubic phase[8,9]. Hafnium and vanadium are two elements which are close neighbors in the periodic table and which raise ρ_n. To summarize a fairly complex investigation somewhat incompletely, we

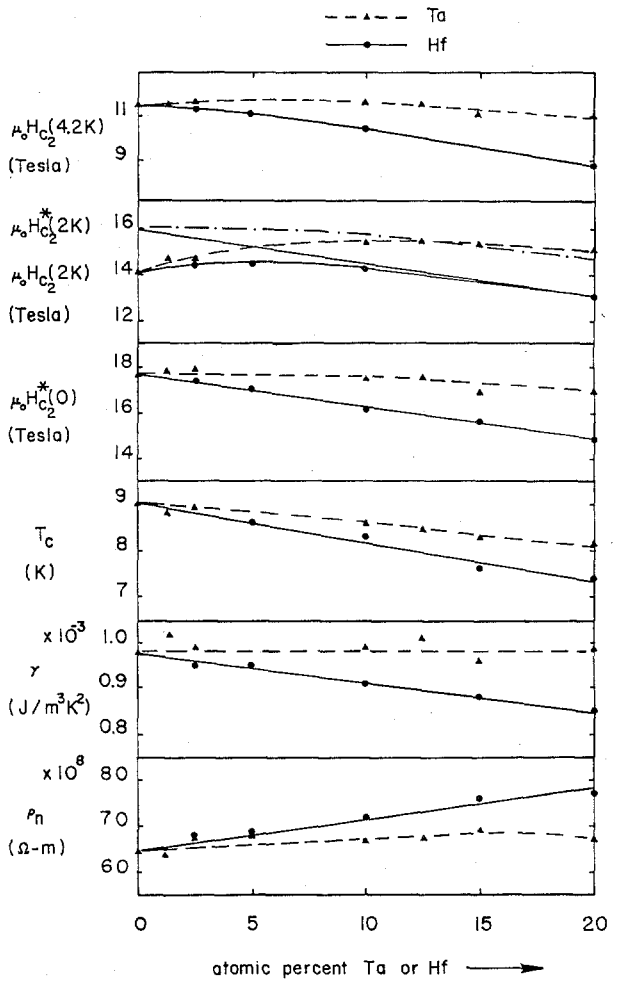

Fig. 6. The variation of ρ_n,γ,T_c, and the theoretical GLAG and experimental upper critical fields, $\mu_0 H_{c2}^*$ and $\mu_0 H_{c2}$ for Nb-Ti-Ta and Nb-Ti-Hf alloys of constant electron to atom ratio (4.35) [9,28].

found, however, that the resistivity increases may be outweighed by decreases in T_c and γ[9,28]. The orbital paramagnetism of the normal state is always important and the degree of spin-orbit scattering which relieves this is therefore crucial to the development of higher upper critical fields. A comparison between Nb-Ti-Ta and Nb-Ti-Hf alloys is shown in Fig. 6. Of the parameters in the GLAG equation, T_c is seen to decline in both cases as Hf and Ta are substituted for Ti and Nb, respectively. γ declines for substitutions of Hf, remaining constant for substitutions of Ta. ρ_n increases for Hf substitutions, remaining approximately constant for Ta substitutions. In both alloy systems, the net effect is to produce decreases in the GLAG value of H_{c2}, $\mu_0 H_{c2}^*(0)$. The decrease is relatively small for Ta, somewhat larger for Hf. What counts practically, however, are the experimental values. In binary Nb-Ti alloys, there is significant paramagnetic limitation and both Hf and Ta, being heavy elements, are efficient removers of the limitation through the means of spin orbit scattering[32].

The relative importance of this increases as the temperature decreases (since, at higher temperatures, the Cooper pairs are thermally disordered). Experimentally, no enhancement is seen in the 4.2K upper critical field of the Nb-Ti-Hf alloys, although there is a small enhancement in the Nb-Ti-Ta system (11.8 T vs 11.5 T). At 2K, the increases become significant, particularly in the Nb-Ti-Ta system (Figs. 7 and 8). The effect of additions of 10-15% of Ta or Hf is to completely remove the paramagnetic limitation (Fig. 6), producing an enhancement of $\mu_0 H_{c2}$(2K) from 14.25 T in the best binary alloy (Nb 46.5w/o Ti) to 15.5 Tesla for a wide range of alloys around Nb 25w/o Ta 43w/o Ti. Although it is not appropriate to discuss the theoretical aspects of these results further here, we should point out that the behavior of these alloys has many features of intrinsic scientific interest that we report on elsewhere[9,28,31].

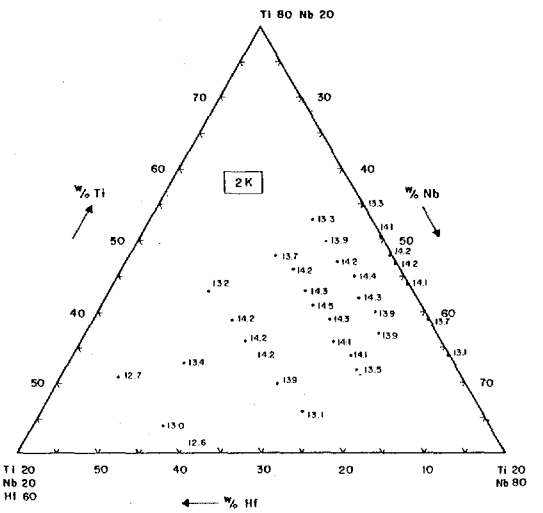

Fig. 7. Experimental upper critical fields at 2K for Nb-Ti-Hf alloys[28,45].

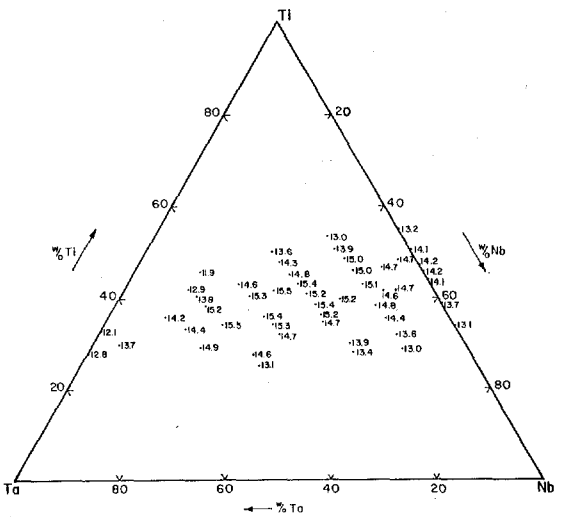

Fig. 8. Experimental upper critical fields at 2K for Nb-Ti-Ta alloys[28,45].

The increases in H_{c2} are obtained even though the T_c of the Nb-Ti-Ta alloy is lower. At high fields, however, the spin-orbit scattering process causes the H_{c2} vs. T curves of the binary and ternary alloy to cross as is shown in Fig. 9[31].These increases in H_{c2} are of considerable practical interest when allied with He II cooling. Industrial fabrication of the Nb 25w/o Ta 43w/o Ti alloy has taken place in the form of a Fermilab design billet which will be incorporated into the General Atomic 12 Tesla test coil[34]. The current densities attained in this alloy take the ductile alloys into at least the 12 Tesla and perhaps the 13 Tesla range, areas where Nb_3Sn hitherto was the only practical alternative. We discuss the current density of this alloy in the next section.

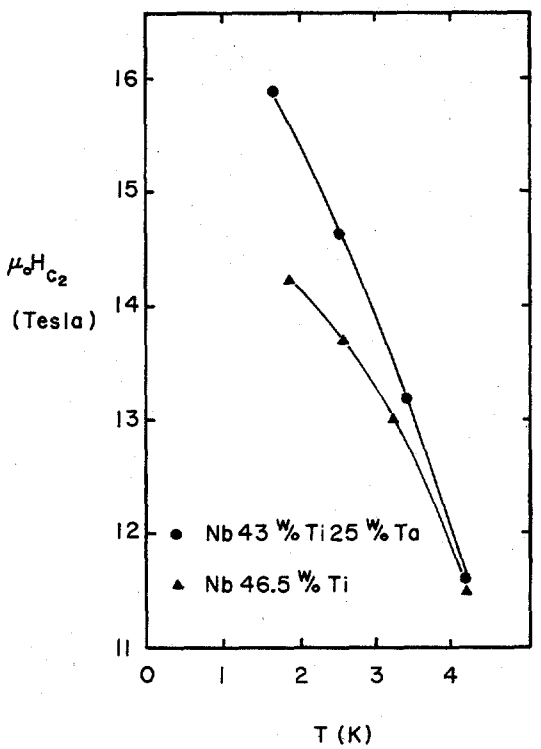

Fig. 9. Critical field versus temperature for Nb 46.5w/o Ti and Nb 43w/o Ti 25w/o Ta[28]

Critical Current Densities

The general foundation for our understanding of the critical current density in Nb-Ti alloys was laid down some 10 years ago in work reported by some of the superconductor manufacturers. For example, Hillmann and his co-workers[35] established the importance of α-Ti precipitation in Nb 50w/o Ti, Neal et al.[36] showed the importance of small sub-band diameter and final size heat treatment in the lower-Ti content single phase alloys such as Nb 42w/o Ti, while Critchlow et al.[37] showed that heat treatments performed at several times the final wire diameter were more effective than those performed at the final size. Each of these observations is still valid - yet there is still widespread secrecy over the fabrication recipe used by each manufacturer and considerable divergence in current density from one design of composite to another and even between remakes of the same design of composite.

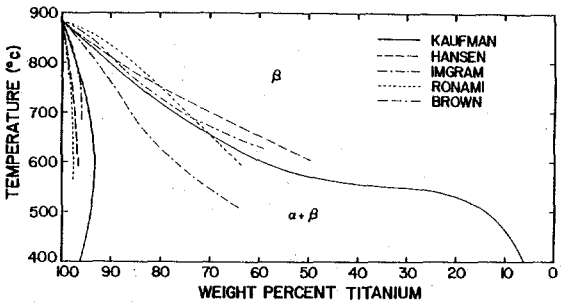

Fig. 10. The α/β phase fields in Nb-Ti[9].

An interesting detail of composite design is the question of alloy composition. Nb 50w/o Ti remains the alloy favored by Vacuumschmelze, while US manufacturers prefer the more Nb-rich, Nb 46.5w/o Ti. As can be seen in Fig. 4, both alloys have optimal H_{c2} values, particularly since the Nb 50w/o Ti alloys are heat treated to produce significant α-Ti precipitation, thus making the matrix composition more Nb-rich. The papers of Hillmann[35] have recognized this for many years but it is interesting to note that Nb 46.5w/o Ti was formulated partly on the basis that fine filament, low AC loss, HEP conductors required single phase alloys in order to avoid break up during drawing. The low temperature portion of the phase diagram of Nb-Ti is shown in Fig. 10. It can be seen how flat the β/α+β phase boundary is in the vicinity of 45-50w/o Ti. This writer's opinion is that the exact composition of the alloy within this range is of less importance than the defect density produced by the fabrication of the alloy. Careful transmission electron microscopy of ours has shown that α-Ti precipitation is crucial to the development of high J_c in Nb 46.5w/oTi, as in Nb 50w/oTi[38,39]. Hillmann has, however, argued that composition is very important, although without giving the processing details to support the argument[40].

When we began our studies of the critical current density in Nb-Ti and its alloys, we were impressed by the diversity of claims made by different authors and manufacturers. The quotation, "There are three kinds of lies: lies, damned lies and statistics" is attributed by the Oxford Dictionary of Quotations to Mark Twain through Disraeli[41]. We feel certain that a modern Mark Twain would have felt compelled to add a fourth category "Lies, damn lies, statistics and critical current densities", to his list. Fortunately there is an ASTM committee battling presently with this problem and we send them our best wishes on their lengthy task[42]. Our comments, though facetious, are, however, meant to have a serious base. The current density can be measured precisely and it is a significant waste of valuable information to overestimate the J_c of practical composites by varying amounts when this information is generally the sole information available to measure the effects of the complex fabrication process used to produce the conductor.

The approach that we took in our investigations was to seek out a representative selection of the

composites being commercially produced in the world, to systematically measure their properties over the field range up to H_{c2} at 4.2K and below and to use transmission electron microscopy (TEM) to characterize their microstructures. Details on 4 of the composites thus investigated are given in Table 2, where it will be noted that there is a significant range of composition, filament size, number etc[26,38,43].

Table 2

Details of the Four Commercial Nb-Ti Composites

	Nb 46.5w/oTi	Nb 50.4w/oTi	Nb 52.7w/oTi	Nb 41w/oTi 15wo/Ta 8w/oZr
Wire Diameter (nm)	0.686	0.60	0.83	0.31
Copper/S.C. Ratio	1.8:1	1.2:1	1.8:1	8.86:1
Number of Filaments	2100	60	180	61
Filament Size (μm)	10	52	38	29
Sub-Band Diameter	455Å	400Å	510Å	415Å
and	+	+	+	+
Microstructural State	α-Ti	α-Ti	α-Ti	α-Ti

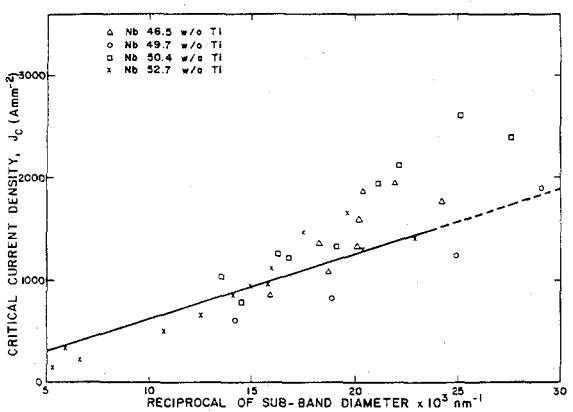

Fig. 11. Critical current density at 5T, 4.2K vs. the inverse sub-band diameter[38]. The solid line is due to Neal et. al.[36].

The TEM examinations revealed structures such as those shown in Fig. 2, where the elongated structure is an array of dislocation sub-band walls 40-50nm apart, introduced by the very large degrees of cold work[21]. Not visible in the microstructure, but of crucial importance to the development of high J_c values, is an array of normal α-Ti precipitates (they are evident in the diffraction pattern, however). An important early investigation was that of Neal et al.[36], who found an inverse relationship between J_c and sub-band diameter in single phase alloys. Their maximum J_c(5T, 4.2K) value was about 1200 A/mm^2, a value that would be considered very low today. A plot of our data shows that the simple inverse dependence no longer holds for high J_c composites, (Fig. 11[38]) since it is now the α-Ti precipitate array which is the larger contributor to the J_c. However, actual data on the density and distribution of the precipitates are sparse[9] and this remains an important area of ignorance, not only because of the effect on J_c but also because of the effect that precipitation has on initiating composite break-up.Critical current density values at 4.2K and 2K measured at a true 10^{-14}Ωm composite resistivity are given in Figs. 12 and 13 and 13 (these should therefore be excepted from Mark Twain's description). It should be emphasized that these curves are not meant to be typical or necessarily characteristic of the alloys, nor, as has been discussed earlier, is the composition necessarily the determining factor in the differences between the composites. Rather it is the overall combination of

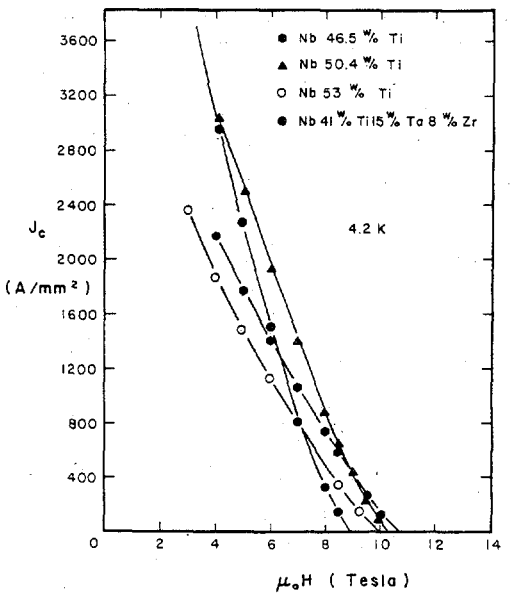

Fig. 12. Current densities of commercial composites at 4.2K[8,26].

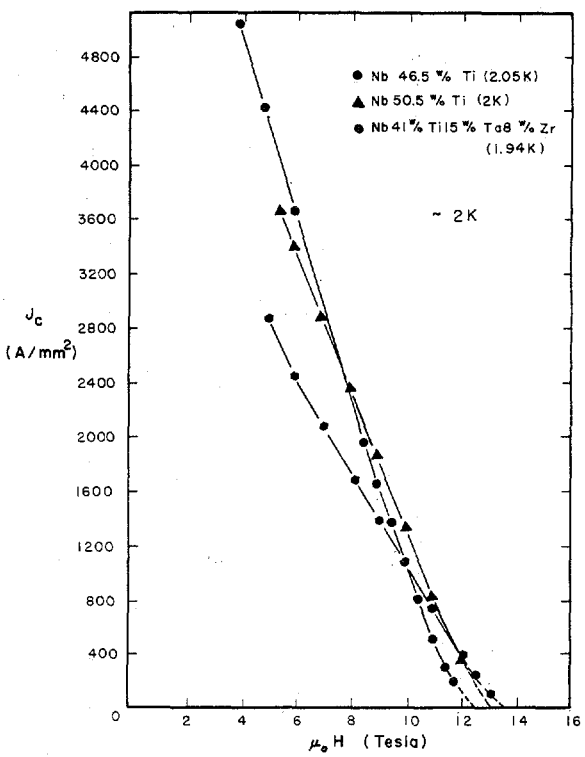

Fig. 13. Current densities of commercial composites at about 2K[9,26].

the alloy composition, the extrusion conditions, the degree of cold work and the heat treatment schedule that determines the J_c within the T_c, H_{c2} envelope provided by the alloy matrix composition. Three points at least are worthy of note:

(i) There is a wide range of J_c value at any given field (eg. J_c(5T, 4.2K) ranges from ~1500 to ~2600 A/mm^2, J_c(8T, 4.2K) from ~400 to 800 A/mm^2).

(ii) The J_c at 2K is substantially larger than that at 4.2K (5T ~ twice, 8T ~ three times).

(iii) The ternary alloy containing Ta and Zr has an extraordinarily high low field, low temperature J_c (>6000 A/mm^2 at 2T, 2K). This may be attributed to the effective nature of the flux pinning α-Ti precipitates when Zr is present.

Table 3

Sub-band Diameters as a Function of Heat-Treatment and Cold-Work in a Fermilab Nb 46.5wt.% Ti FM Composite (West and Larbalestier, [39].

Sub-band Diameter (nm)	Cold Area Reduction Ratio	Heat Treatment	α-Ti Precipitation
69	255	none	none
63	3742		
53	5878		
46	7533		
98	255	1 hr/300°C	none
84		3/300	none
86		30/300	possible
92		100/300	slight
87		1/375	
		3/375	
		30/375	possible
111		100/375	definite
77		1/400	
94		3/400	possible
166		30/400	definite
129		100/400	

For none of the above composites were heat treatment and fabrication schedules available. In general terms, however, the schedules are well-known; a typical treatment being to extrude by 16-20:1 area reduction ratio at 500-550°C, cold draw to 3-5 times the final wire diameter and heat treat for 20-200 hours at 350 to 400°C. More details have been given in earlier reviews by us[8,9]. What actually happens during the heat treatment is revealed in a recent study of ours on a Fermilab composite[39]. First, the unstable sub-band structure shows substantial growth and only after some considerable time does the α-Ti precipitation process begin. (Table 3) The first of these processes tends to drive down the J_c, the second to drive it back up. The heat treatment takes place at a very low temperature with respect to the melting point (~0.3) and the diffusion processes needed to permit the α-Ti precipitation occur within the defect structure of the sub-band walls. The sub-band diameter is determined by the degree of cold work; the greater the degree of cold work, the finer is the sub-band diameter. The importance of cold-work is therefore its effect on sub-band diameter and on the kinetics of the sub-band growth/α-Ti precipitation process during heat treatment. It is here that the great complexity in the processing and optimization of Nb-Ti lies. The small amount of published data on these points is quite insufficient to permit quantitative predictions and is the reason why composite development proceeds by trial and error optimization. Further microstructural evaluation of practical composites is vital. Figure 14 exemplifies one of the complexities of microstructual examination. Two apparently similar microstructures are shown from a final size Fermilab composite. One has a J_c (5T, 4.2K, 10^{-14}Ωm) value of 366A/mm^2, one a value of 1540A/mm^2. There is a small difference in the sub-band diameter, 51 versus 44nm, but this is quite insufficient to explain the difference in J_c.

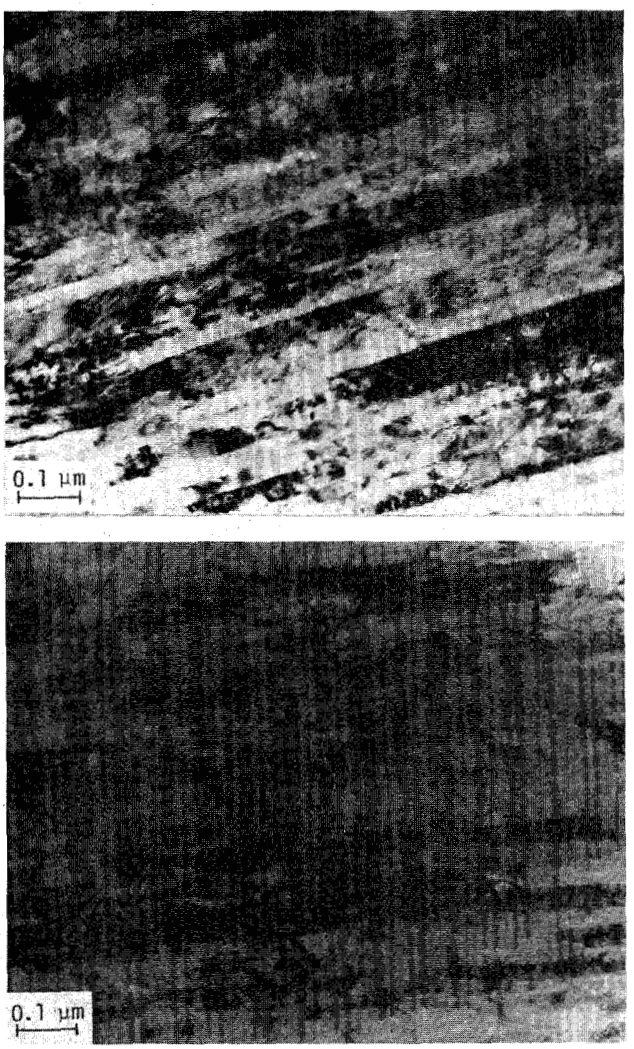

Fig. 14. Transmission electron micrographs of Fermilab composites at final size. The upper has received no heat treatment, the lower 160 hours at 375°C[21,39]. See text for details.

The crucial difference is that the higher J_c, finer sub-band material received a heat treatment of 160 hours at 375°C at 5-1/3 times the final wire size. This heat treatment almost doubled the sub-band diameter but produced α-Ti precipitation and the subsequent cold work in the presence of the precipitates refined the sub-band diameter to 44nm, below that of the sample which received no heat treatment and contained no precipitates. The J_c of the heat treated sample was 1540 A/mm^2 and a subsequent heat treatment at final size (3hrs/300°C) which produced no change in

sub-band size or presumably the α-Ti precipitate distribution raised the J_c further to 1670 A/mm^2. A fuller discussion of these and other factors affecting the J_c may be found in a recent review[9].

Scaling Behavior

Another useful tool for assessing the quality of a superconducting composite can be the intelligent use of the scaling laws first observed by Fietz and Webb[44]. These authors noted that the field dependence of the volume pinning force F_p could be scaled by H_{c2}, according to the empirical expression,

$$F_p = J_c \times B = \mu_0 H_{c_2}^{n}(T)\ f(h) \qquad (2)$$

where n is an empirically determined exponent having values from about 1.7 to 2.5 for Nb-Ti[9,47] and f(h) is the shape of the pinning force curve. During the development of the Nb-Ti-Ta alloys for the 12 Tesla program[34], we made extensive use of this relationship[26,45]. The J_c data plotted in Figs. 12 and 13 is replotted in scaling form in Figs. 15 and 16. Figure 15 shows the magnitudes of the pinning force in the different commercial composites, where of course the maximum pinning force F_{pmax} varies widely depending on the degree of optimization. Note, however, that the position of F_{pmax} is rather independent of composite, occurring at about $0.45H/H_{c2}$ for all. When the pinning force is itself normalized, as in Fig. 16, the curve shapes are seen to be very similar and do not depart greatly from a h(1-h) dependence ($h=H/H_{c2}$).

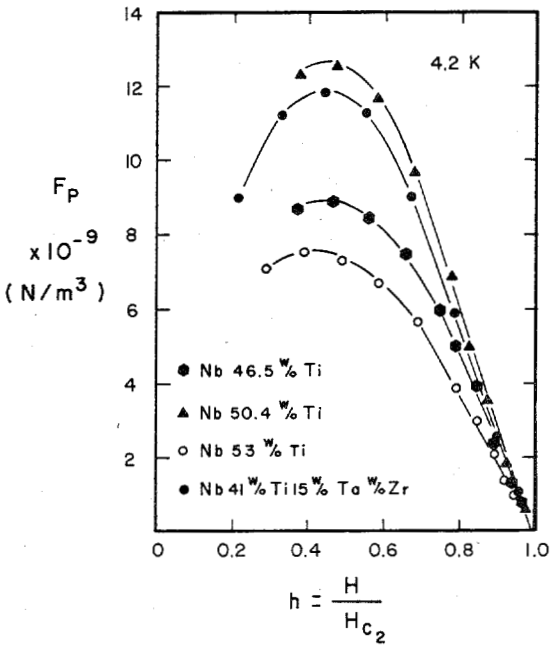

Fig. 15. Pinning force (J_cxB) vs. reduced field at 4.2K for the four Nb-Ti multifilamentary composites whose J_c data are given in Fig. 12[8,26].

There are a number of points to be made about the scaling behavior. First, the shape of the curve is extremely sensitive to the details of the interaction between the vortex lattice (which may be amorphous, however, in such a strong pinning microstructure) and the microstructure. Although we do not yet know how to sum the interactions between the individual fluxoids and their pinning sites, we do know that the more efficient the pinning, the lower in reduced field h will the peak in f(h) occur[46]. Thus the position of F_{pmax} is a significant guide to the success of optimization in a given composite and is a substantial argument for making current density measurements over at least the mid-field range where the peak in F_p occurs (say 3 to 7 Tesla for Nb-Ti at 4.2K) when new composite designs are in fabrication.

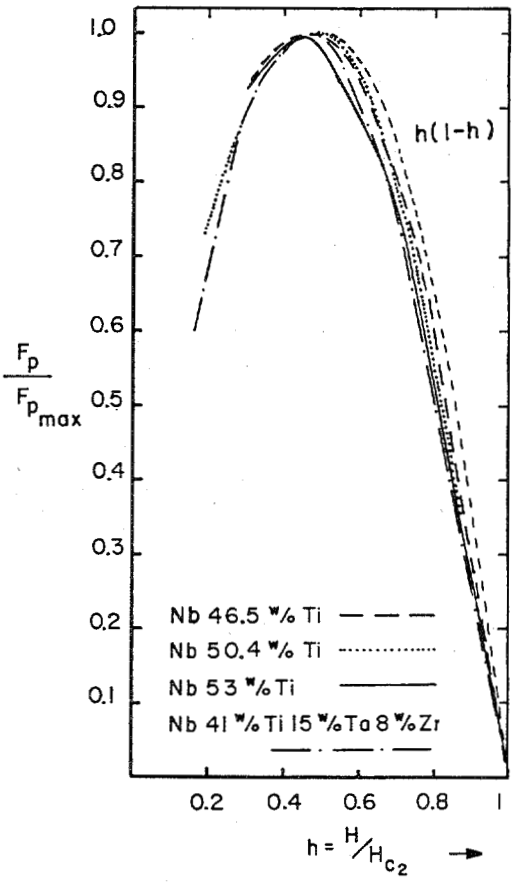

Fig. 16. Superimposed reduced pinning curves for four commercial Nb-Ti filamentary composites[26].

A second point is that the scaling relations can be practically very useful in saving a lot of testing. While neither the exponent in Eq. 2 nor f(h) can be explicitly predicted in advance (though n appears always to have a value of 2 to 2.1 for optimized conductors[26,47]), the temperature scaling of f(h) is excellent [see ref. 26]. Moreover the high field shape of f(h) at greater than 0.75h is linear to a very high degree of accuracy[26]. Both these points enable the low temperature and the high field J_c to be

predicted to good order.

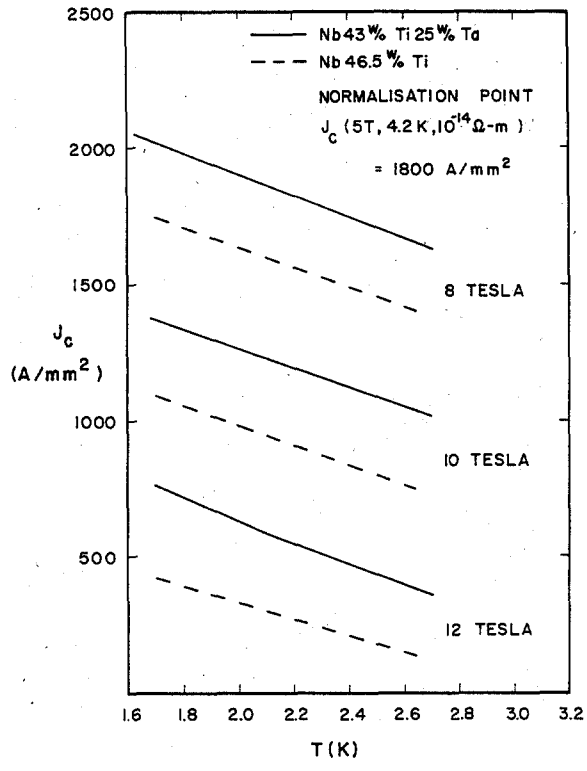

Fig. 17. Comparison of the predicted J_c values at 8,10 and 12 Tesla for Nb 46.5w/o Ti and Nb 43w/o Ti 25w/o Ta composites (Courtesy D.G. Hawksworth).

Such a procedure was followed by us for the Nb 43w/o Ti 25w/o Ta alloy[26]. In advance of the manufacture by MCA of a multifilament billet, we scaled the high field J_c, using Eq. 2 and our measurements of the temperature dependence of H_{c2} in our 30gm sample of the Nb-Ti-Ta alloy and the MCA Nb 46.5w/o Ti standard product[26,48]. Our prediction of the 12 Tesla, 2K J_c fell within 10% of the value actually obtained by MCA[48]. Figure 17 shows that there is a considerable critical current margin for the ternary alloy and that the temperature margin of the Nb-Ti-Ta alloy over Nb 46.5w/o Ti is about 0.7K. Further optimizations will certainly improve the current density. In fact, when the pinning force curve of the first industrial samples of the ternary alloy[48] are compared to those of Nb 46.5w/oTi[28], the peak in F_p is seen to occur at a much higher field (~0.55 H_{c2}, Fig. 18). This strongly suggests that insufficient α-Ti precipitation has occurred during heat treatment, a conclusion also supported by the relatively low 5T J_c of this particular composite. Further developments of this alloy are discussed by Segal et al.[49] in a paper at this conference.

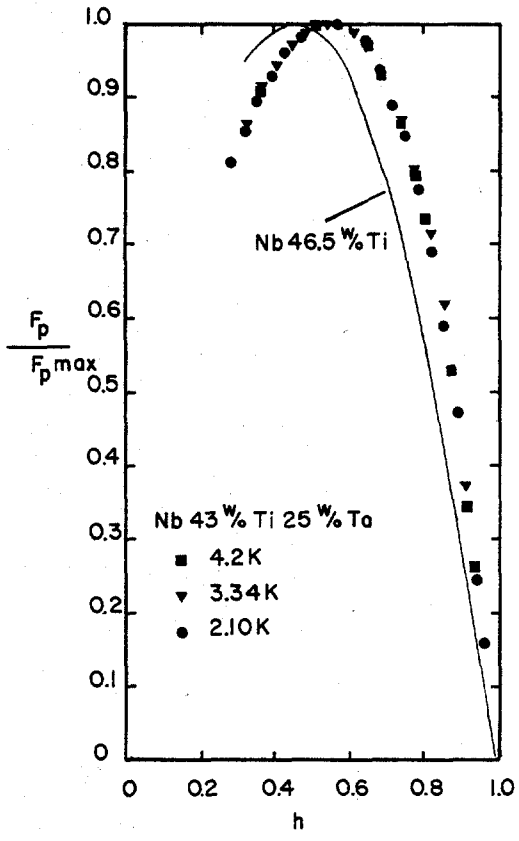

Fig. 18. Reduced pinning force curves for Nb 46.5w/o Ti and Nb 43w/o Ti 25w/o Ta multifilamentary composites[28].

Table 4

Costs and Components for a Fermilab Energy Saver Billet (Data Courtesy of R. Remsbottom [50]).

Extrusion diameter	250 mm
Final size	0.68 mm dia.
Number of filaments	2070
Filament diameter	8-10 μm
Cu:Nb-Ti ratio	1.8:1 nominal
Weight of Nb-Ti per billet	60 kg
Weight of Cu tubing	96 kg
Weight of Cu extrusion can (nose cone + tail = 36.6 kg)	90 kg
Total weight of extrusion	247 kg
Cost of Nb-Ti at $198/kg	$11,880
Cost of Cu tubing at $6.60/kg	636
Cost of extrusion can	1,644
	$14,160

Raw material cost = $57.38/kg
Processing cost at 3¢/ft = 9.84¢/m = $33.86/kg
Total cost = $57.38 + $33.86 = $91.24/kg

Fabrication and Industrial Considerations

The reliable and economical fabrication of composites is the job of industry and there have been many considerable achievements by the industry in recent years. An interesting perspective is provided by the

Fermilab composite, since it has been made in great quantity, by a variety of manufacturers and some reasonably firm data is available on its costs and properties. The raw material is high purity Nb 46.5w/o Ti (the principal impurities are O and Ta at 1000 ppm max, all others being less than 200 ppm) and OFHC Cu. The cost of production in 1980 was $91.25/kg (composed of a raw material cost of $57.40 and a production cost to 0.68 mm dia. strand of $33.85). The cost breakdown is shown in greater detail in Table 4[9,50].

The current density in the final strand has varied from time to time and manufacturer to manufacturer but is typically about 1800-2000A/mm^2 (5T, 4.2K, $10^{-14}\Omega m$), although somewhat higher values have recently been obtained[51]. A magnet builder really wants ampere turns, however, so that one appropriate normalization factor is the cost per A.m. The Fermilab conductor is in fact a 23 strand compacted Rutherford cable and, including a cabling cost of $1.41 per meter, the price per A.m for different field values are shown in Table 5. Values are given at both 4.2 and 2K so that one of the cost factors involved in a He-II system analysis may be quantified. Of course, most conductors do not have the production history of the Fermilab conductor behind them and some need to be considerably more complex. However, some idea of baseline cost is surely very useful in the scoping stage of conductor design.

Table 5

1980 Costs of Fermilab Cable per Kilo-amp·m[50].

Single strand costs	26.5c/m
23 strand cost	$ 6.09/m
Cabling cost	$ 1.41/m
Total cost	$ 7.50/m

Field	Current Density		Cost per kA.m	
	4.2K	2K	4.2K	2K
4 Tesla	2200	3200	$1.11	$0.77
5	1800	2800	1.36	0.87
6	1400	2400	1.75	1.02
8	750	1700	3.26	1.44
10	150	1050	16.32	2.33
12	----	400	----	6.12

The above values are based on a nominal critical current of 5500A at 5T and 4.2K, corresponding to a $J_c(10^{-14}\Omega m)$ value of 1800A/mm^2.

A recent introduction to the U.S. market by Wah Chang has been Nb derived from pyrochlore ore. The principal feature of the use of this ore is that the Nb is likely to have a higher residual Ta content than that made from columbite ore, perhaps leading to residual Ta levels of as much as 5000 ppm in Nb and Nb-Ti[52]. Experiments on model alloys[9,53] of Nb-Ti suggest that there is little cause for concern, though the whole question of small impurity levels (such as Fe) is really not well understood. Significant economic gains have been predicted from the use of pyrochlore Nb[53] and their current introduction is being monitored to see whether these predictions turn out to be true.

A final point to be considered in the fabrication of Nb-Ti conductors is the question of conductor assembly. Large magnets run at currents of one to tens of thousands of amperes. High current densities require large area reductions (~10^4:1), while initial extrusions are presently limited to about 30cm in diameter. Although there have been examples of large, monolithic conductors (eg. MFTF), the general tendency is to assembly by cabling or braiding, as in the Fermilab cable or Brookhaven Isabelle braid. The question of changes in current density which occur during the assembly of optimized strands can still be extremely vexing. Optimized strands require α-Ti precipitates but subsequent over-working of such strands can produce excessive breakage or reduction in current density. This is an important area where little understanding yet exists but whose practical importance is considerable.

An alternative approach to conductor build up has recently been developed at Airco for the Elmo Bumpy Torus and Tore-II conductors[54]. Individual strands of a standard conductor, such as the Brookhaven Isabelle design, are assembled together near their final size and continuously wrapped with a Cu strip which is automatically welded to form a continuous sheath. A final drawing and heat treatment produces a high current conductor having the degree of cold work belonging to a small diameter conductor (Fig. 19).

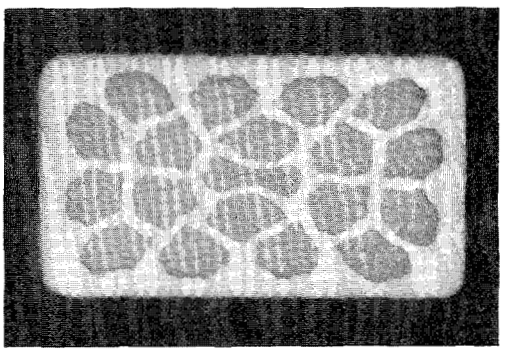

Fig. 19. Compacted monolith conductor for EBT made of 19 Brookhaven Isabelle design strands (Courtesy of S.O. Hong).

IV. NIOBIUM-TIN

The basic conductor design for Nb_3Sn is more complex than for Nb-Ti because there are now four components in the composite, the tin supply, the Nb, the diffusion barrier and the high purity stabilizing Cu. The intrinsic brittleness of Nb_3Sn requires reaction at final size and diffusion rates are so slow that filaments of much less than 10μm are needed in order to keep reaction times reasonable. The large number of components in the composite and the small filament size tends to exacerbate the problems of co-processing; filament sausaging and irregular filament shape are constant problems to be avoided.

If bronze is used for the tin supply, many anneals are needed to avoid cracking the bronze and some reaction to Nb_3Sn occurs at each anneal, perhaps posing problems if filaments of less than 5μm are needed. For the present, the only composites of practical importance are the conventional bronze route composites containing Nb embedded in a bronze matrix, generally Cu 13w/o Sn. In essence, their design remains essentially similar to the first prototype magnet conductors introduced at the 1974 Applied Superconductivity Conference[55,56]. Many different variants of composite designs have since been produced and evaluated.

Although the capability for the production of Nb_3Sn composites is in principle well-established there are still large uncertainties regarding the intrinsic properties of filamentary (FM) Nb_3Sn composites. Particular problems are the fact that the diffusion layers of Nb_3Sn generally have a composition gradient across them, leading to inhomogeneous superconducting properties[23-25], and that the properties of Nb_3Sn are very sensitive to stress and thus show marked effects, which may be very variable on a local scale, resulting from the compression exerted by the surrounding bronze[13,14].

For these and other reasons there is as yet little general agreement on what the basic envelope of properties to be obtained from a FM Nb_3Sn composite should be and why present composites show such variable properties. An index of this situation, which particularly strikes the present writer, is the range of bronze to Nb ratios chosen by different manufacturers, values ranging from 4.6 to 2:1 being manufactured[57-59].

In order to restrict these comments to those of reasonable extent, the principle discussion will bear on bronze route FM Nb_3Sn. A wider perspective can be obtained from a number of the more general reviews, already noted in the introduction[10-20].

Basic Properties and Their Characterization

A logical place to begin is in the selection of starting bronze and Nb needed to form the Nb_3Sn. Knowledge of the required qualities and purities of these constituents is of course of considerable economic importance yet there are still important areas of disagreement. There is, at least in the USA, no general agreement yet on whether the 13w/o bronze should be air or vacuum cast and on what the tolerance for oxygen is. Experience has been variable. The successful AERE bronzes were all air melted[55,59,60] as is the bronze for the LCP conductor[61] but Livermore has favoured vacuum casting as producing a more ductile bronze[62]. The oxygen solubility in pure Cu is extremely low (<10 ppm at 700°C)[63], (although it is very mobile) but there is much unpublished "folk-lore" that oxygen solubility is higher in bronze and exerts significantly deleterious effects on both the fabricability and the final properties of the composite. High purity Sn and Cu are generally used for the bronze but again there appears to be little agreement on the required purity or the deleterious impurities which are being guarded against in selecting high purity starting elements. There are fewer concerns about the purity of the Nb, since the electron beam melting process is inherently capable of purifying down to very low levels, but even here the requirements of co-processing may require special selection of the Nb.

The selection of input purities must be judged both against the test of fabricability through multiple extrusion (generally required because of the small size and large filament number), wire drawing, multiple annealing and the properties obtained after the composite is reacted at final size. Characterization of the final size properties is not necessarily straightforward, however.

Chemical analysis of thin layers of 1-2μm or less is not at all routine since, although most laboratories have access to standard electron probe microanalyzers and they are frequently used to probe Nb_3Sn layers, their limit of resolution lies between 1 and 2μm. Recourse must therefore be made to more exotic techniques such as Auger electron spectroscopy (AES). Recent work in our laboratory[24,25] has shown that, with careful correction procedures, the composition and impurity profile can be obtained on a scale of about 0.1μm (Fig. 20). These studies have produced at least two interesting points, the first being that the Sn concentration profile is relatively flat, thus ensuring good superconducting properties over most of the layer. Most of the required concentration gradient thus appears to occur close to the Nb/Nb_3Sn interface.

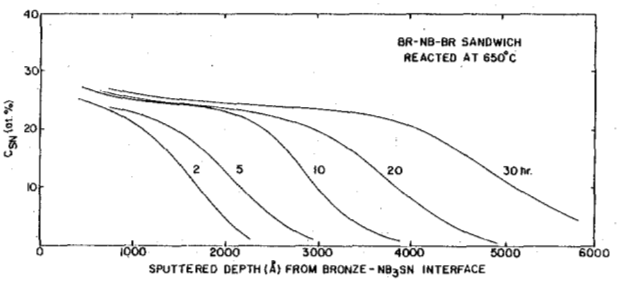

Fig. 20. Auger electron spectroscopy sputter profiles for the Sn peak obtained on diffusion grown Nb_3Sn layers. The zero sputtered depth is the bronze-Nb_3Sn interface. The Sn concentration drops to zero as the Nb core is reached. (Courtesy of D.B. Smathers)

The second point relates to the reduced properties of thin layers. Thin layers (<200nm) are seen to be high in O and possibly C too, reducing the Sn content below stoichiometry and depressing the superconducting properties[25]. This is clear evidence for the deleterious effect of O on Nb_3Sn properties, though it is unclear whether the O source originated in the bronze or was derived from the O originally adsorbed on the surface of the Nb rods.

A detailed analysis of the capabilities of magnetization measurements for revealing the structure of thin layers of Nb_3Sn has been presented by Evetts

et al.[23] and their discussion of the capabilities and limitations of the basic electrical and magnetic characterization experiments is invaluable for workers seeking to use such techniques to reveal basic information about thin layers[23].

Transition Temperatures and Upper Critical Fields

Due to the surrounding matrix and the axial compressive strain imposed on the Nb_3Sn, there exists a significant depression of both the T_c and H_{c2} of FM Nb_3Sn[10,13]. Since the depression depends on such factors as the bronze to Nb ratio and the yield strength (and residual composition) of the bronze, it is necessary to remove the bronze in order to be able to assess the fundamental quality of the Nb_3Sn.

The T_c depression is well established to be parabolic in the axial strain[13], reaching a maximum of about 1.2K for large bronze to Nb ratios. Practical ratios (2.5-4.5:1) reduce T_c by about 0.5K. When the bronze is etched off, maximum T_c values reach about 18K, 0.1-0.3K below the maximum recorded for pure Nb_3Sn. This may be due to Cu incorporation in the layer, residual inhomogeneities or strains or other presently unknown factors.

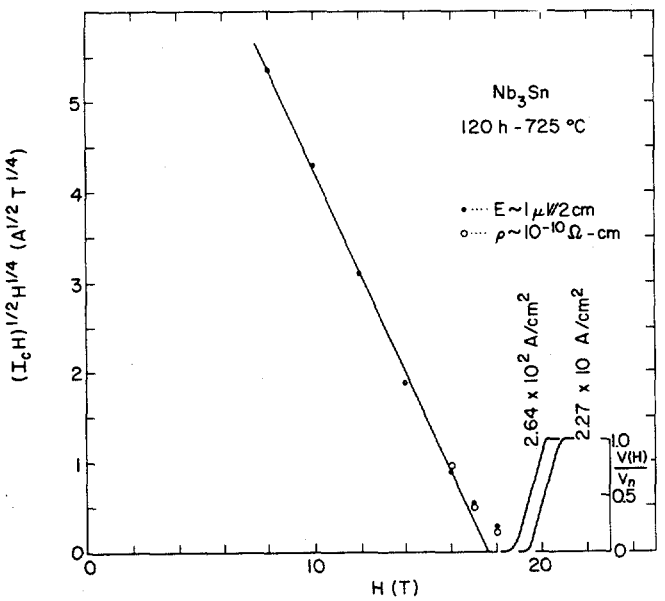

Fig. 21. A plot of $J_c^{1/2}H^{1/4}$ vs. H for a monofilamentary Nb_3Sn wire which was heat treated at 725°C for 120h, indicating the extrapolated H_{c2} and the low current density H_{c2}[64].

Although there is good agreement on the T_c values to be expected, the question of H_{c2} is more unclear. Few workers have made measurements at other than 4.2K and even fewer have had access to fields greater than $\mu_0 H_{c2}(4.2K)$. An extrapolation function is, therefore, needed in order to derive the H_{c2} from lower field J_c measurements. This question has been extensively discussed by Suenaga and Welch[10,64]. The Kramer function $J_c^{1/2}B^{1/4}$ is found to be a linear function of the J_c over much of the field range (~10 to 18T) but increasing divergences are noted thereafter, high field tails existing to 22T or higher (Fig. 21). If the pinning center density is higher than is normal for FM Nb_3Sn (eg. in irradiated material or very small filament in situ conductors), a $(1-a_0\sqrt{\rho}\ )$ multiplying correction factor must be used to linearize the J_c plot (where a_0 is the fluxoid separation and ρ the density of flux pinning sites.) However, even for field ranges where this scaling relation works well, the magnitudes of the scaling parameters are shown to be incompatible with some of the basic physical properties of Nb_3Sn. The physical basis of the Kramer model as applied to Nb_3Sn thus appears doubtful although it may be useful as an empirical tool[64]. To the uncertainty in H_{c2} generated by the use of an extrapolation function, we may add the additional uncertainties of the possibilty of a low temperature cubic-tetragonal phase transformation and a general lack of measurements of γ and ρ_n, data which are needed to fit the behavior of Nb_3Sn to the basic GLAG and WHH theories (Eq. 1)[32,33]. Measurements of ρ_n in FM Nb_3Sn are really not feasible, due to the irregularity of the cross-section (Fig. 22)[66] and the presence of an unreacted Nb core and γ can therefore not be deconvoluted from the slope (dH_{c2}/dT) at T_c, which is proportional to $\rho_n\gamma$.

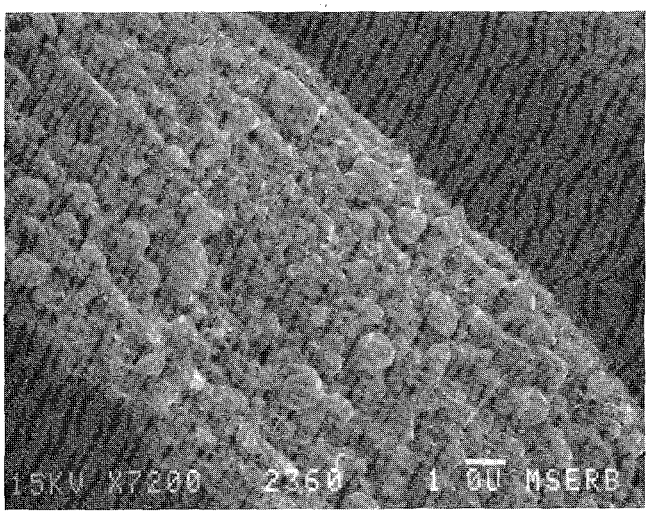

Fig. 22. Scanning electron micrograph of a single filament from a multifilament Nb_3Sn composite. The layer was reacted to completion at 780°C for 168hrs.

Recent work on electron beam evaporated films[33,66] and bulk samples[20,67] has indicated that there should be considerable scope for improvement in the upper critical field. Figure 23 is taken from the work of Orlando et al.[66] on thin films deposited on sapphire substrates (ρ_n and γ can then be determined and the properties compared to

theory[33]). Peak $\mu_0 H_{c2}$ values are seen to attain 29T at 0 K or ~25T at 4.2K, for a T_c value, however, of about 16K and a relatively high ρ_n of ~25μΩcm. These values are some 3 to 5 Tesla higher than those commonly observed for FM Nb_3Sn.

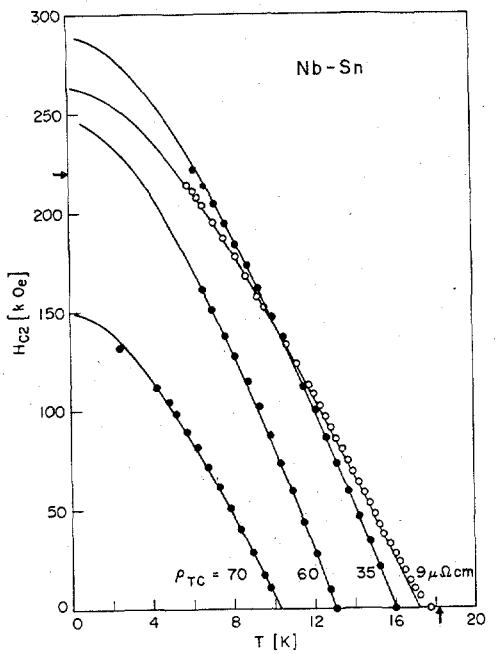

Fig. 23. Critical fields of Nb-Sn with different normal state resistivities ρ_{Tc}. As the resistivity ρ_{Tc} increases, T_c decreases but H_{c2} goes through a maximum[66].

A possible explanation for the depression of H_{c2} and the large stress sensitivity of H_{c2} has been advanced in a number of recent publications[68-72]. The principal proposal is that the unstressed composite leaves the Nb_3Sn in substantially the tetragonal state, tensile strain then causing growth of the higher H_{c2} cubic phase[67,69]. A number of groups are active in this area and conclusive evidence should soon be available to support or deny this explanation.

The literature on 3rd element additions to Nb_3Sn is rather extensive and we refer to Suenaga for recent reviews[8,9]. Ta, Zr, Hf and Ti can increase H_{c2} (as judged by critical current extrapolations) towards the 25T level[74]. At present the reasons for the increases are not clear; they may reflect either an intrinsic increase in H_{c2} due to changes in the properties which go into Eq. 1 or a modification of the cubic/tetragonal phase balance so as to produce more of the cubic high H_{c2} phase[69,71,72].

Critical Current Density

Critical current densities in FM Nb_3Sn are found to vary quite widely and particularly above 12T, the J_c is found to fall off rather rapidly. When the pinning force of presently optimized FM Nb_3Sn is compared to that of Nb-Ti (Fig.24), the Nb_3Sn is seen to be rather under-optimized at high fields[57]. This probably reflects the fact that significant pinning is produced only by grain boundaries. The differing shapes of the two curves does draw attention to the considerable gains that could be made if Nb_3Sn could be optimized to the same extent as Nb-Ti.

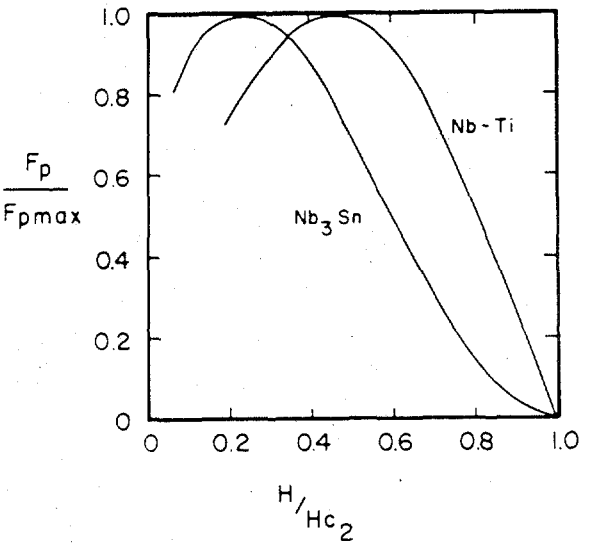

Fig. 24. Pinning force curves for optimized FM Nb_3Sn and NbTi conductors [57].

From a fundamental point of view, the J_c in the layer is the crucial quantity but the large number of filaments, their small size and irregular shape makes the determination of the cross-sectional area difficult. Practically, it appears more reasonable to normalize the critical current to the original bronze + Nb package needed to make the Nb_3Sn and this is almost invariably the method used today. This will however obscure changes in layer J_c: for example it is perfectly feasible for the J_c in the layer to decline as the reaction proceeds, while the overall J_c increases as the total cross-sectional area increases.

The comments of Mark Twain, recalled earlier, are probably even more applicable to measurements made on Nb_3Sn. Resistive voltages are more common in resistive transition plots, both because of the longer current transfer lengths in the resistive bronze and because of damage to the filaments. Both effects lead to broadened transitions, making the criterion used to define J_c important. The strain sensitivity of J_c can also lead to misleading results and it has also been shown that the form on which the wire is mounted can exert a significant influence on the J_c[75]. The long barrel sample reacted and soldered to a stainless steel cylinder probably remains the most desirable test but it is also demanding in terms of the diameter of reaction furnace, ease of mounting and time required for test[76]. Since many reaction treatments are generally required to map out the characteristics of a composite, there is a tendency to accept simpler sample configurations yielding more questionable data.

Suenaga[10,11] has recently made an extensive summary of the J_c values found in the literature, both for conventional FM Nb_3Sn and its in situ variants. The results are shown in Figs. 25 and 26.

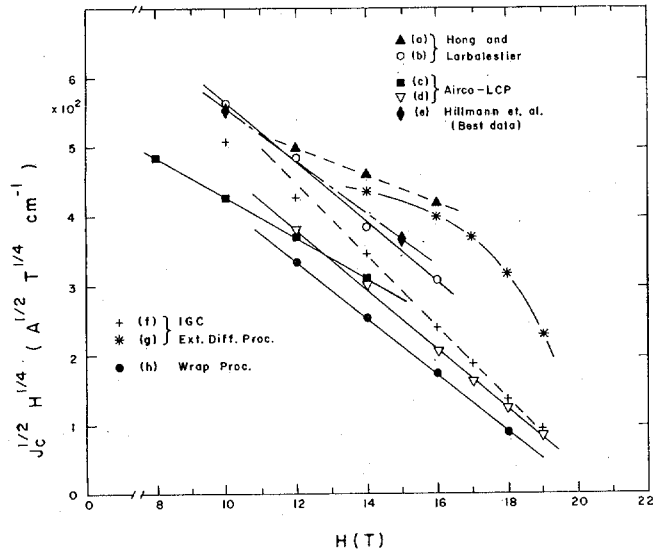

Fig. 25. A comparison of J_c in commercially processed multifilamentary wires plotting $J_c^{1/2}H^{1/4}$ vs H.

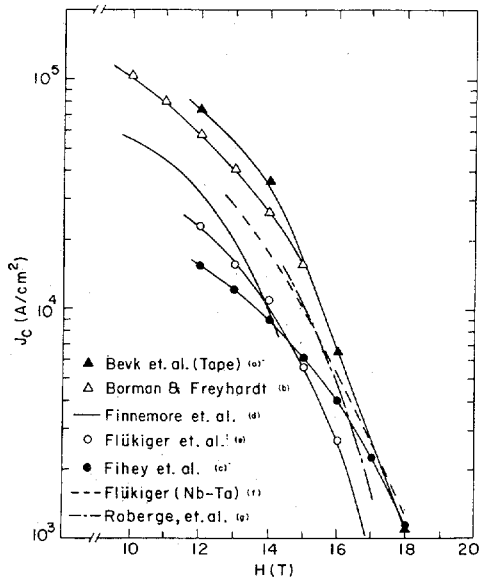

Fig. 26. A comparison of J_c vs. H in experimental Nb_3Sn wires produced by various in situ processes [11].

The diversity of values is obvious. It is also interesting to note that in situ J_c values, at least below about 12 Tesla, appear to be fully comparable to bronze route values.

The question of optimization through correct choice of composite design, filament size and reaction treatment remains largely unanswered. Perhaps the best characterized commercial composite remains the original AERE design[55,59,76]. The J_c values of this composite were particularly good below about 14 Tesla (Fig. 27), falling off above this field due to the reduced H_{c2} produced by the high bronze to Nb ratio (4.6:1). Comparison to the properties of 2 lower ratio composites (2.7:1 and 3:1) appears to suggest a cross-over at around 14 Tesla, the lowest ratio composite being best at high fields, as expected from its lower precompression. More surprising is its lower J_c at lower fields - unless this may be related to the varying extent of the cubic to tetragonal phase transformation with varying bronze to Nb ratio. However, these comparisons must remain provisional since the 3 composites came from different manufacturers, had somewhat different fabrication histories, starting bronzes, etc. and are in no sense the product of a controlled production series. All the full line values are for 6 to 8μm diameter filaments, while the dashed line is for a nominally identical remake of the initial AERE composite with 3μm dia. filaments[77].

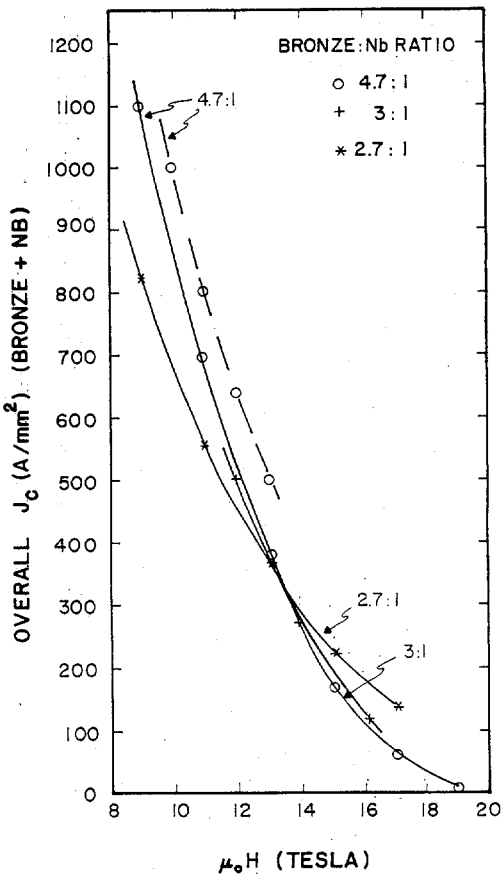

Fig. 27. J_c vs $\mu_0 H$ for several Nb_3Sn composites of different bronze to Nb ratios[77].

The absolute values of the J_c are comparatively good, reaching ~850 A/mm² at 10T (higher in finer filaments, a trend confirmed elsewhere[78]) and 550

A/mm^2 at 12T. An interesting conclusion to be drawn from a study of this composite is that there may be some economic, as well as technical gain, to be derived from the higher bronze to Nb ratio composites, since bronze is appreciably cheaper than Nb.

A final emphasis with respect to the question of J_c in FM Nb_3Sn is that we are still very uncertain about what a reasonable limiting value of J_c should be and that there remains much that is curious about the reaction characteristics of particular composites. It is to be hoped that, as standard designs of composite become more widely available, as much effort will be put into their characterization as goes into their fabrication.

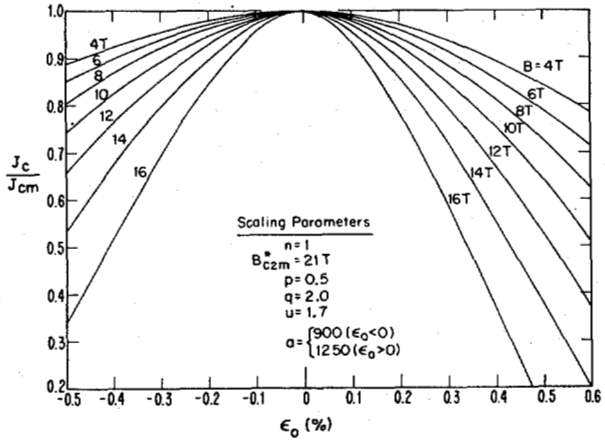

Fig. 28. Relative critical-current density J_c/J_{cm} as a function of intrinsic strain $\varepsilon_0(\equiv\varepsilon-\varepsilon_m)$ for different magnetic fields evaluated using Eq. (3) and the typical set of scaling parameters indicated in the figure [79].

Strain Effects

The strain sensitivity of Nb_3Sn is of such fundamental importance to its application that a large amount of work has been performed and, as may be seen from the recent reviews of Welch[13] and Ekin[14], the subject appears to be phenomenonologically well understood. Unless the bronze to Nb ratio is very low[58], uniaxial tensile strain is found to increase T_c, H_{c2}, and J_c, until the point at which the residual axial strain on the Nb_3Sn reaches zero. For practical composites, this requires strains of 0.3 to 0.6%. The magnitude of the increase in J_c is dependent on field and precompression, increasing with both parameters. Ekin[79] and Rupp[80], in particular, have stressed the utility of strain scaling, finding that data on a wide variety of commercial composites can be fitted to the equation[79]:

$$\frac{J_c}{J_{cm}} = \left[\frac{H_{c_2}(\varepsilon)}{H_{c_{2m}}}\right]^{n-p} \left[\frac{1-H/H_{c_2}(\varepsilon)}{1-H/H_{c_{2m}}}\right]^{q} \qquad (3)$$

where the subscript m refers to the maximum value obtained at zero intrinsic strain, while n, p and q are empirically determined exponents of values ~1, ~0.5 and 2, respectively. The utility of such a set of scaling relations is obvious and an example is shown in Fig. 28.

The preceding scaling behavior describes the elastic behavior of the Nb_3Sn and ceases to be valid when filament cracking occurs. An interesting feature of FM Nb_3Sn is that its strain tolerance is remarkable for a brittle material, since by the conventional rule of thumb, the Nb_3Sn should fracture at a strain of 0.2% or less. The strain tolerance arises both from the precompression (the Nb_3Sn must of course be taken into tension before it can crack) and the filamentary nature of the phase. Simple elastic stress analysis shows that the stress concentration at the root of a notch has the value $2(c/\rho)^{1/2}$, where c is the crack half length and ρ the radius of curvature at the notch root. ρ is fixed, being of the order of the interatomic spacing in a brittle material, leaving the crack length as the important variable. Notches must be expected in brttle materials (see, for example, the irregular reaction in Fig. 22) and without plastic flow to blunt the notch, some cracking must always be expected. The upper limit to the crack length is clearly the fiber diameter. For a 1 μm diameter filament, the stress concentration is about 45, rising to ~1400 for a 1 mm dia. filament. Fine filaments thus have higher failure stresses (and strains) and the improved behavior of even finer filaments is confirmed in the in situ and special fine filament Cu-Nb composites[17,81], where failure strains as high as 1 to 2% have been observed.

Although most experiments have been performed in uniaxial tension, the case of bending is also important. Luhman et al.[82] have shown that the bend tolerance is not as high as the uniaxial strain tolerance. The reason for this is that the bronze on the outer tension side of the neutral axis yields before that on the inner circumference, forcing the neutral axis towards the center of curvature and preferentially damaging the outer filaments. However, for both types of stress, the fracture is progressive rather than catastrophic and bend strains of ~0.5% appear feasible in practical conductors.

As a practical point, we may note that the first coils to be wound of FM Nb_3Sn performed very well at stresses of up to 150 MPa[59]. Their quench currents were substantially (35 to 50%) greater than the short sample critical currents but since these were obtained in the early 1970's when training was expected to reduce the behavior of the magnets the results seemed improbable and were not published until some 3 years later[59]. In fact, the earliest experiments on the tensile properties of individual wires proved that it was easier to damage the wires in isolation than was the case when they were wound into coils, and reacted in place. The prospects for magnet use are therefore very good. Since the maximum peak design strain seldom exceeds 0.2% in a large magnet, Nb_3Sn has in principle a safety margin of 2 to 3 in strain. The problem of utilizing the Nb_3Sn is thus a problem of ensuring that this strain will not be exceeded or of

providing appropriate relief (extra cooling etc.) for regions where it may be.

Fabrication Considerations

Although the usage of FM Nb_3Sn does not yet approach that of Nb-Ti, there is now a considerable forward committment to its use in large magnets and large scale production lines have been set up to produce it. We have already remarked on the large diversity of present conductor designs and the extent, therefore, to which any one design can be considered standard is doubtful. The design to be most widely produced in the near future is, however, the LCP strand at Airco (Fig. 29). Over 100 extrusions of this design will be made and much will be learnt about the effect of process variables if good characterizations are made of different billets of this conductor[83].

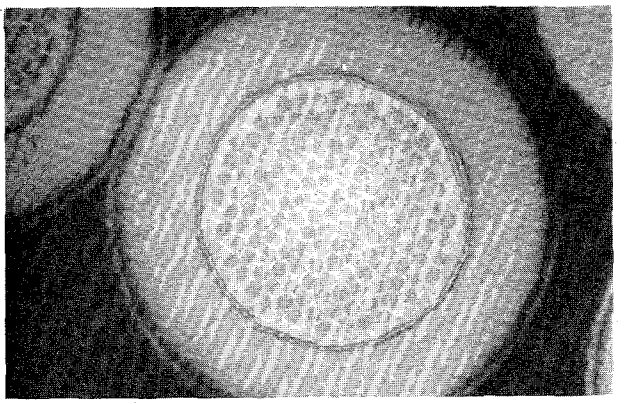

Fig. 29. The Airco LCP conductor. (Courtesy of P. Sanger)

Alternative processing routes of a variety of designs have been proposed and wire produced on a small scale. Amongst these we may cite the external diffusion route, applied both to conventionally stacked Cu-Nb billets and in-situ billets, the use of Sn-rich compounds in place of bronze as the Sn source and the extensive work on in-situ composites, using both casting and powder extrusion routes. We refer to recent reviews[10,11,15-17] for more details of these processes. This diversity of approach emphasizes that Nb_3Sn of good quality can be produced in a variety of ways, even if none of these alternative processes has yet achieved commercialization.

Although cost advantages are frequently cited in support of alternative routes to FM Nb_3Sn, it should be realized that these arguments really rest on a very uncertain foundation. The reason for this is that we do not yet have firm cost data (that is published at least) for bronze route Nb_3Sn. A start might, however, be made by dividing the costs into raw material and fabrication categories. Since the raw material costs tend to be similar from process to process, this may indicate whether much is to be gained from alternative processing. The data in Tables 4 and 5 enable such a comparison to be made for Nb-Ti but I am not aware of any comparable data for Nb_3Sn.

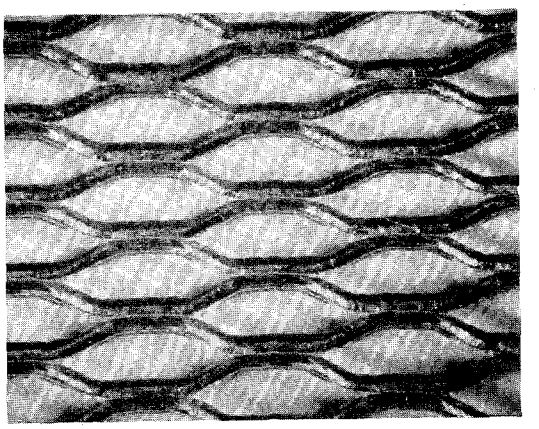

Fig. 30. Expanded Nb sheet used in the Jelly Roll Nb_3Sn composite shown in Fig. 31. (Courtesy of W.K.McDonald.)

One variant of the bronze process recently proposed by Wah Chang does however deserve some mention in view of its interesting properties and apparent production simplicity. Nb foil is slit on a conventional slitter used to produce expanded mesh (Fig. 30) and rolled in a "jelly or Swiss roll" with bronze sheet, so as to produce a multiply connected filament network. After wrapping with a diffusion barrier and a Cu stabilizer, the billet is compacted and then extruded and drawn in a conventional manner[84]. Recent reports of the AC loss of this composite (Fig. 31) suggest that it acts much more like a conventionally stacked composite with disconnected filaments than a multiply connected in situ composite[85]. The prospects for this Wah Chang process may be considerable, therefore, in view of the elimination of much billet stacking and multiple extrusion work.

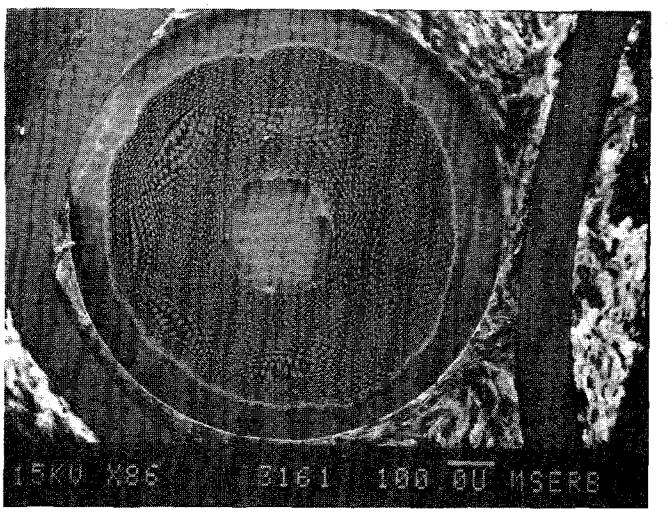

Fig. 31. The Jelly Roll Nb_3Sn composite of Wah Chang. (Courtesy of W.K. McDonald.)

ACKNOWLEDGEMENTS

A number of people deserve my thanks for help in the preparation of this review. I am particularly indebted to members of my own group for discussions and assistance; particularly David G. Hawksworth, David B. Smathers and David L. Moffat. The use of unpublished thesis work of David G. Hawksworth and David B. Smathers is also gratefully acknowledged. Recent discussions with Dr. Masaki Suenaga on the properties of Nb_3Sn were also of great assistance.

Finally I am pleased to acknowledge the support for our research provided by the Department of Energy, Office of Fusion Energy and Energy Storage Systems.

REFERENCES

1. Workshop Panel Session, "Superconductors for Magnets: Frontiers of Technology," Session WA-1, this conference.
2. D.B. Montgomery, Proceedings of the 6th Symposium on Eng. Problems of Fusion Research, IEEE Publication 75CH1097-5-NPS, p. 122 (1975).
3. M.A. Green, paper DD-1, this conference.
4. Advances in Cryogenic Engineering 26 10, Plenum Press (1981).
5. Filamentary A15 Superconductors, editors M. Suenaga and A.F. Clark, Plenum Press (1980).
6. Superconducting Materials, editors S. Foner and B.B. Schwartz, Plenum Press (1981).
7. Proceedings of the 1980 Applied Superconductivity Conference, IEEE Trans. MAG. 17 1 (1981).
8. D.C. Larbalestier, Ref. 4.
9. D.C. Larbalestier, Ref. 6.
10. M. Suenaga, Ref. 6.
11. M. Suenaga, Ref. 7.
12. H. Hillmann, Ref. 6.
13. D.O. Welch, Ref. 4.
14. J.W. Ekin, Ref. 6.
15. D.K. Finnemore, Ref. 4.
16. S. Foner, Proceedings of the 8th Symposium on Engineering Problems of Fusion Research, IEEE Publication 79CH1441-5-NPS, p. 230 (1979).
17. R. Roberge, Ref. 6.
18. J. Bevk, M. Tinkham, F. Habbal, C.J. Lobb and J.P. Harbison, Ref. 7, p. 235.
19. A.I. Braginski and G.R. Wagner, Ref. 7, p. 243.
20. R. Flukiger, Ref. 6.
21. A.W. West, University of Wisconsin, unpublished.
22. A.W. West and R.D. Rawlings, J. Mat. Sci. 12, 1862 (1977).
23. J.E. Evetts, J.R. Cave, R.E. Somekh, J.P. Stanton and A.M. Campbell, Ref. 7 p. 360.
24. D.B. Smathers and D.C. Larbalestier, Ref. 4, p. 415.
25. D.B. Smathers and D.C. Larbalestier, Ref. 5, p. 143.
26. D.G. Hawksworth and D.C. Larbalestier, Ref. 16, p. 249.
27. E.J. Kramer, J. Appl. Phys. 44, 1360 (1973).
28. D.G. Hawksworth, Ph.D. thesis, University of Wisconsin (1981).
29. N.E. Alekseevski, O. Ivanov, I.I. Rayevskii and N.V. Stepanov, Soviet Physics Doklady 12, 9 (1968).
30. T. Horiuchi, Y. Monju and N. Nagai, J. Jap. Inst. Met. 37, 8 883 (1973).
31. D.G. Hawksworth and D.C. Larbalestier, to be published.
32. N.R. Werthamer, E. Helfand and P.C. Hohenberg, Phys. Rev. 147, 295 (1967).
33. T.P. Orlando, E.J. McNiff, Jr., S. Foner and M.R. Beasley, Phys. Rev. B19 4545 (1979).
34. J.S. Alcorn, J.R. Purcell, W.Y. Chen and Y.H. Hsu, Ref. 7 p. 642.
35. I. Pfeiffer and H. Hillmann, Acta Met. 16 1429 (1968).
36. D.F. Neal, A.C. Barber, A. Woolcock and J.A.F. Gidley, Acta Met 19 143 (1971).
37. P.R. Critchlow, E. Gregory and B. Zeitlin, Cryogenics 11 3 (1971).
38. A.W. West and D.C. Larbalestier, Ref. 4.
39. A.W. West and D.C. Larbalestier, Ref. 7, p. 65.
40. H. Hillmann, Int. Disc. Meeting on Flux Pinning in Superconductors, Sonnenberg, W. Germany (1974) p. 235.
41. Oxford Dictionary of Quotations, Oxford University Press (1979) p. 187.
42. A.S.T.M. committee, F. Fickett, NBS Boulder, CO, private communication.
43. K.F. Hwang and D.C. Larbalestier, IEEE Trans. Mag. 15, 1 p. 400 (1979).
44. W.A. Fietz and W.W. Webb, Phys. Rev. 178 p. 657 (1969).
45. D.G. Hawksworth and D.C. Larbalestier, Ref. 7 p. 49.
46. E.J. Kramer, J. Electronic Matls. 4, 839 (1975).
47. R.G. Hampshire and M.T. Taylor, J. Phys. F 2, 89 (1972).
48. H.R. Segal, T. M. Hrycarj, Z.J.J. Stekley, T.A. deWinter and K. Hemachalem, Ref. 16, p. 274.
49. H.R. Segal, Z.J.J. Stekley, T.A. deWinter and K. Hemachalem, paper BB-10, this conference.
50. R.H. Remsbottom, University of Wisconsin, private communication.
51. B.A. Zeitlin, Intermagnetics General Corporation, private communication.
52. R.J. Marsh and W.K. McDonald, Teledyne Wah Chang, private communication.
53. C.W. Curtis and W.K. McDonald, IEEE Trans. MAG. 13, 769 (1977).
54. E. Gregory, E. Adam, S. Hong, W. Marancik. P. Sanger, C. Spencer, paper FB-1, this conference.
55. D.C. Larbalestier, P.E. Madsen, J.A. Lee, M.N. Wilson and J.P. Charlesworth, IEEE Trans. MAG 11, 247 (1975).
56. E. Gregory, W.G. Marancik and F.T. Ormand, IEEE Trans. MAG 11, 295 (1975).
57. D.C. Labalestier, IEEE Trans MAG 15, 209 (1979).
58. D.C. Larbalestier, J.E. Magraw and M.N. Wilson, IEEE Trans. MAG 13, 462 (1977).
59. D.C. Larbalestier, Proc. MT-6, Alfa Publ. Co., Bratislava 1080 (1978).
60. J.A. Lee and C.A. Scott, ibid, p. 35, Ref. 5.
61. P.A. Sanger, E. Adam, E. Ioriatti and S. Richards, Ref. 7, p. 666.
62. R. Scanlan, Lawrence Livermore National Lab, private communication.
63. V.M. Horrigan, Met. Trans A 8A, 785 (1977).
64. M. Suenaga and D.O. Welch, Ref. 5, p. 131.
65. D.B. Smathers, unpublished work.
66. T.P. Orlando, J.A. Alexander, S.J. Bending, J. Kwo, S.J. Poor, R.H. Hammond, M.R. Beasley, E.J. McNiff, Jr.; and S. Foner, Ref. 7, p. 368.
67. H. Devantay, J.L. Jorda, M. DeCroux, J. Muller and R. Flukiger to appear in J. Mat. Sci.
68. R.W. Hoard, R.M. Scanlan, G.S. Smith and C.L. Farrell, Ref. 7, p. 364. 314o
69. R. Flukiger, Report KFK Oct.198o,Kernforschungs-zentrum Karlsruhe
70. D.M. Kroeger, D.S. Easton, C.C. Koch and A. DasGupta, Ref. 5, p. 205.
71. R. Roberge, H. LeHuy, S. Foner, to appear in Phys. Lett.
72. R. Flukiger, W. Specking, B. Schmidt and E. Springer, paper GB-6, this conference.
73. S. Foner and E.J. McNiff, Jr., Appl. Phys. Letts. 32, 122 (1978).

74. H. Sekine and K. Tachikawa, Appl. Phys. Letts. 35, 472 (1979).
75. H. Hillman, H. Pfister, E. Springer, M. Wilhelm and K. Wohlleben, Ref., p. 17.
76. S.O. Hong and D.C. Larbalestier, IEEE Trans MAG 15, 784 (1979).
77. S.O. Hong and D.C. Larbalestier, unpublished work.
78. M.S. Walker, J.M. Cutro, B.A. Zeitlin, G.M. Ozeryansky, R.E. Schwall, C.E. Oberly, J.C. Ho and J.A. Woollam, IEEE Trans MAG 15 80 (1979).
79. J.W. Ekin, Ref. 7, p. 658.
80. G. Rupp, Ref. 7, p. 1099.
81. S.F. Cogan, D.S. Holmes, R.M. Rose, J. Appl. Phys. 51 4332 (1980).
82. T. Luhman, D.O. Welch, M. Suenaga, Ref. 7, p. 662.
83. P. Sanger, Airco, private communication.
84. W.K. McDonald, Wah Chang, private communication.
85. S.S. Shen, Oak Ridge National Lab, private communication.